

Study of the ${}^9\text{Be}(p, \alpha){}^6\text{Li}$ reaction via the Trojan Horse Method

S. Romano^{1,2,a}, L. Lamia^{1,2}, C. Spitaleri^{1,2}, C. Li¹, S. Cherubini^{1,2}, M. Gulino^{1,2}, M. La Cognata^{1,2}, R.G. Pizzone¹, and A. Tumino^{1,2}

¹ Laboratori Nazionali del Sud - INFN, Catania, Italy

² Dipartimento di Metodologie Fisiche e Chimiche per l'Ingegneria, Università di Catania, Catania, Italy

Received: 1 July 2005 /

Published online: 13 March 2006 – © Società Italiana di Fisica / Springer-Verlag 2006

Abstract. The Trojan Horse Method has been applied to the ${}^2\text{H}({}^9\text{Be}, {}^6\text{Li}\alpha)$ three-body reaction in order to investigate the ${}^9\text{Be}(p, \alpha){}^6\text{Li}$ two-body reaction, which is involved in the study of light element abundances (lithium, beryllium and boron). A coincidence measurement was performed in order to identify the presence of the quasi-free mechanism in the three-body reaction, needed for the application of the method. The astrophysical $S(E)$ -factor was extracted and compared to direct data. No information about electron screening effects can be extracted due to the poor resolution of the indirect data.

PACS. 24.10.-i Nuclear reaction models and methods – 26.20.+f Hydrostatic stellar nucleosynthesis

1 Introduction

In recent years the abundances of light elements lithium, beryllium and boron (LiBeB) have been increasingly used as diagnostics between different scenarios for primordial or stellar nucleosynthesis. As reported in [1], beryllium primordial abundances can provide a powerful test to discriminate between homogeneous and inhomogeneous primordial nucleosynthesis. Moreover, the study of beryllium abundances in young stars, together with lithium and boron, can provide a strong test for understanding stellar structure and discriminate between possible non-standard mixing processes in stellar interiors [2]. In both stellar and primordial environments, however, LiBeB are mainly destroyed by proton-capture reactions via the (p, α) channel with a Gamow energy E_G ranging from 10 keV (for stellar nucleosynthesis) to 100 keV (for primordial nucleosynthesis). These energies are low if compared with the Coulomb barrier E_C usually of the order of MeV, thus implying the reactions take place via tunnel effect with an exponential decrease of the cross section to nano or pico barn values. The behavior of the direct cross sections are usually extrapolated at the astrophysical interest region from higher energies by using the definition of the astrophysical factor

$$S(E) = E \cdot \sigma(E) \cdot \exp(2\pi\eta) \quad (1)$$

(where η is the Sommerfeld parameter) which varies smoothly with energy. Nevertheless this extrapolation procedure can introduce some uncertainties due, for example,

to the presence of unexpected subthreshold resonances or electron screening effects [3].

However, in recent years, many indirect methods [4, 5, 6, 7, 8, 9, 10] have been developed in order to extract the $S(E)$ -factor without extrapolations. In particular the Trojan Horse Method (THM) [8, 9, 10] represents a powerful tool which selects the quasi-free (QF) contribution of a suitable three-body reaction under appropriate kinematical conditions. The energy in the entrance channel of the three-body reaction is chosen well above the Coulomb barrier to extract the two-body cross section at astrophysical energies free of Coulomb suppression. In the present paper we present the results of the study of the two-body ${}^9\text{Be}(p, \alpha){}^6\text{Li}$ reaction, obtained through the application of THM to the three-body ${}^2\text{H}({}^9\text{Be}, {}^6\text{Li}\alpha)$ reaction.

2 The Trojan Horse Method

The basic idea of the THM [8, 9, 10] is to extract a two-body $a + b \rightarrow c + d$ reaction cross section from the QF contribution of a suitable three-body $a + x \rightarrow c + d + s$ reaction. Here the x nucleus shows a strong $b \oplus s$ cluster structure and, in the Impulse Approximation (IA) description, only b interacts with a , whereas s is considered to be a spectator to the virtual two-body reaction.

The Plane Wave Impulse Approximation (PWIA) leads to a factorization of the three-body reaction cross section:

$$\frac{d^3\sigma}{dE_c d\Omega_c d\Omega_d} \propto KF \left(\frac{d\sigma}{d\Omega} \right)^{off} \cdot |G(\mathbf{p}_s)|^2, \quad (2)$$

^a e-mail: romano@lns.infn.it

where KF is a kinematical factor, $(d\sigma/d\Omega)^{off}$ is the off-energy-shell differential cross section for the two-body $a(b,c)d$ reaction and $|G(\mathbf{p}_s)|^2$ is the s momentum distribution in x . Under these assumptions, if $|G(\mathbf{p}_s)|^2$ is known (KF is calculated), a quantity which is proportional to the two-body cross section can be extracted from a measurement of the three-body $d^3\sigma/dE_c d\Omega_c d\Omega_d$ cross section.

The above-mentioned assumptions and the validity tests carried out from the data analysis are fully discussed in [10] and references therein.

Moreover in the THM approach [9,10] the initial projectile velocity is compensated for by the binding energy of particle b inside x . Thus the two-body reaction can be induced at very low relative energies. If the incoming energy E_a is chosen high enough to overcome the Coulomb barrier in the entrance channel of the three-body reaction, both Coulomb barrier and electron screening effects are negligible in the two-body THM data. The cluster b is brought into the nuclear interaction region and the x nucleus is considered as a Trojan Horse.

We stress that in view of the various approximations involved in the THM and in particular of the assumption that off-energy-shell effects are negligible, one cannot extract the absolute value of the two-body cross section. However, the absolute value can be obtained through normalization to the direct data available at energies above the Coulomb barrier.

Moreover, as already mentioned, the THM data are not affected by electron screening. Therefore, once the behavior of the absolute bare $S_b(E)$ -factor from the two-body cross-section is extracted, a model-independent estimate of the screening potential U_e can be obtained from comparison with the direct screened $S(E)$ -factor.

The aim of the present experiment was to extract the cross section of the ${}^9\text{Be} + p \rightarrow {}^6\text{Li} + \alpha$ reaction after selecting the QF contribution of ${}^9\text{Be} + d \rightarrow {}^6\text{Li} + \alpha + n$ reaction. The deuteron was used like trojan horse nucleus, due to its $p \oplus n$ structure [11]; in this framework the proton acts like participant while the neutron is the spectator to the virtual two-body reaction.

3 Experimental procedure

The experiment was performed at the Laboratori Nazionali del Sud in Catania. The SMP Tandem Van de Graaf accelerator provided a 22 MeV ${}^9\text{Be}$ beam which was accurately collimated in order to have a spot diameter of about 2 mm and intensities up to 2–5 pA. A deuterated polyethylene target (CD_2) of about $190 \mu\text{g}/\text{cm}^2$ was placed at 90° with respect to the beam direction. A silicon ΔE - E telescope was placed at about 70 cm from the target with an angle of about 45° for a continuous monitoring of the target thickness during the experiment. The particle detection was performed by using two silicon ΔE - E telescopes, with a position-sensitive detector (PSD) as E . The telescopes were placed at opposite sides with respect to the beam direction at a distance from the target $d = 25$ cm. The detection angular ranges were 11.5° – 25.5° (telescope devoted to ${}^6\text{Li}$ detection) and 14.5° – 28.5°

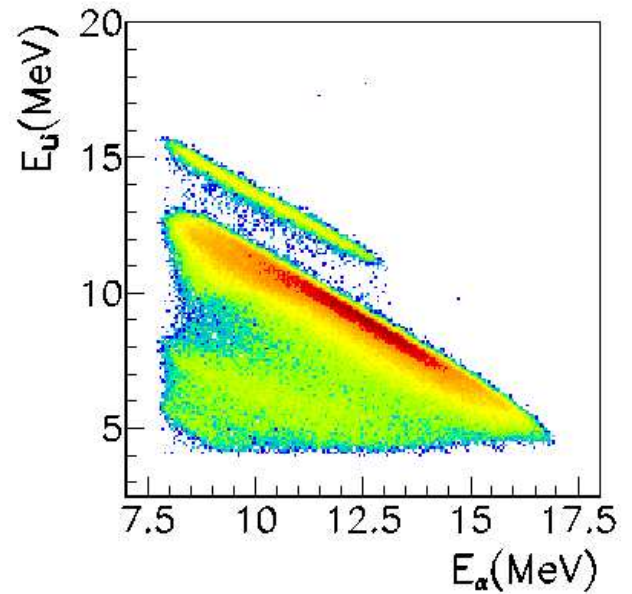


Fig. 1. Experimental kinematic locus E_{Li} vs. E_α for the coincidence events.

(telescope for ${}^4\text{He}$ detection). The displacement of the experimental setup was chosen by means of a Monte Carlo simulation in order to cover the whole QF angular range. The trigger for the event acquisition was given by the coincidence of two particles hitting the two PSDs respectively. Energy and position signals for the detected particles were processed by standard electronics together with the coincidence relative time and sent to the acquisition system for on-line monitoring of the experiment and data storage for the off-line analysis.

In order to perform position calibration, grids with a number of equally spaced slits were placed in front of each PSD. A correspondence between position signal from the PSDs and detection angle of the particle was then established. Energy calibration was performed by means of a standard three-peak α source and α and ${}^6\text{Li}$ particles from ${}^{12}\text{C}({}^6\text{Li}, \alpha){}^{14}\text{N}$ and ${}^{12}\text{C}({}^6\text{Li}, {}^6\text{Li}){}^{12}\text{C}$ reactions.

4 Data analysis

4.1 Three-body reaction identification

After the position and energy calibration, Li and α particles detected in coincidence were selected with the standard ΔE - E technique. The kinematic locus (E_{Li} vs. E_α) (fig. 1) was reconstructed in very good agreement with the simulation. Moreover the experimental Q -value spectrum for the three-body reaction was reconstructed under the assumption of mass number 1 for the undetected third particle. The result is shown in fig. 2, where it is evident a peak centered at about -0.1 MeV according to the expected theoretical value. The results of fig. 1 and fig. 2 make us confident on the identification of the three-body reaction exit channel. Events below the peak in the

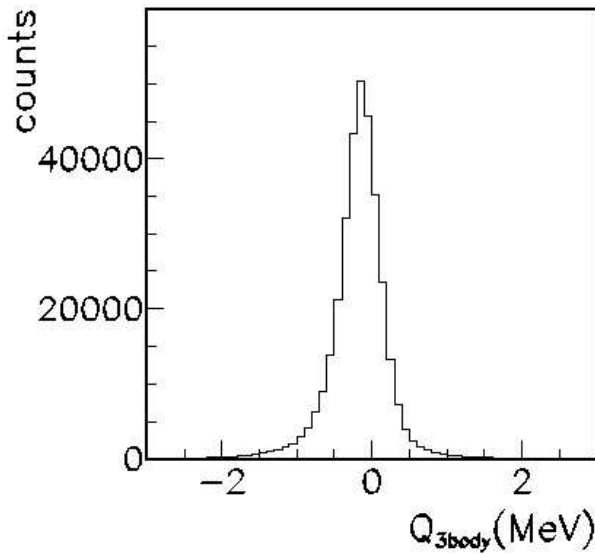


Fig. 2. Experimental Q -value spectrum for the three-body reaction ${}^9\text{Be} + d \rightarrow {}^6\text{Li} + \alpha + n$, with cuts in the kinematical locus in fig. 1.

Q -value spectrum (fig. 2) were selected for the further analysis.

4.2 QF mechanism identification: neutron momentum distribution

According to the theory of the THM [9,10] the energy of ${}^9\text{Be}$ was chosen to overcome the Coulomb barrier in the entrance channel of the three-body reaction. This means that both Coulomb and electron screening effects are negligible in the two-body reaction data. Thus, the term $(d\sigma/d\Omega)^{off}$ in eq. (2) represents the nuclear part of the differential cross section for the virtual two-body reaction ${}^9\text{Be}(p,\alpha){}^6\text{Li}$ that in post collision prescription occurs at an energy

$$E_{cm} = E_{6\text{Li}-\alpha} - Q_{2b}, \quad (3)$$

where $E_{6\text{Li}-\alpha}$ is the ${}^6\text{Li}-\alpha$ relative energy and Q_{2b} is the two-body Q -value.

In order to reconstruct the neutron momentum distribution $|G(\mathbf{p}_s)|^2$, a small ${}^6\text{Li}-\alpha$ relative energy window (about 100 keV) was selected. In such a small energy windows the $(d\sigma/d\Omega)^{off}$ can be considered constant. Thus the experimental $|G(\mathbf{p}_s)|^2$ distribution was extracted by dividing the three-body coincidence yield by the kinematic factor. The result is compared with the theoretical one in fig. 3. The agreement between experimental and theoretical momentum distribution represents a very strong check for the existence of the QF mechanism in the present data.

4.3 Validity tests for the THM and the astrophysical $S(E)$ -factor

After the identification of the QF mechanism only events with spectator momentum $|P_s| < 30 \text{ MeV}/c$ were considered.

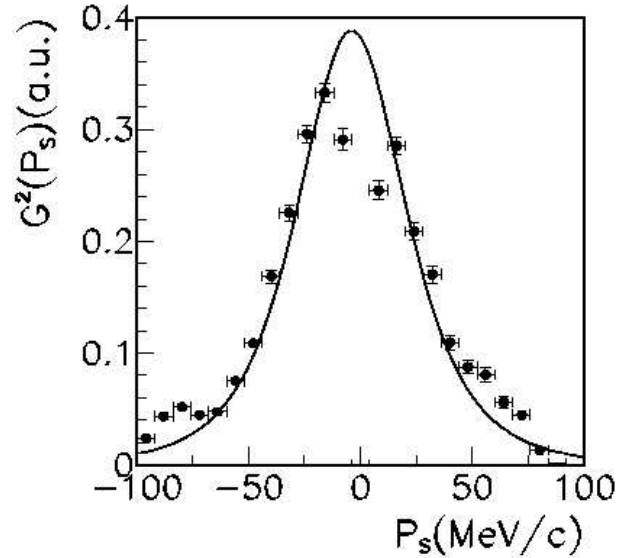


Fig. 3. Comparison between experimental (dots) and theoretical Hülthén function (solid line) for the neutron momentum distribution. Error bars are due to the statistical error.

A first test of validity of the THM approach is represented by the comparison between the indirectly extracted angular distributions and the direct behavior. The relevant angle in order to get the indirect angular distributions, *i.e.* the emission angle for the alpha-particle in the ${}^6\text{Li}-\alpha$ center of mass system, can be calculated according to the relation [12]

$$\theta_{cm} = \arccos \frac{(\mathbf{v}_p - \mathbf{v}_t) \cdot (\mathbf{v}_C - \mathbf{v}_\alpha)}{|\mathbf{v}_p - \mathbf{v}_t| |\mathbf{v}_C - \mathbf{v}_\alpha|}, \quad (4)$$

where the vectors $\mathbf{v}_p, \mathbf{v}_t, \mathbf{v}_C, \mathbf{v}_\alpha$ are the velocities of projectile, transferred proton, and the outgoing ${}^6\text{Li}$ and α -particles, respectively. These quantities can be calculated from their corresponding momenta in the laboratory system, where the momentum of the transferred particle is equal and opposite to that of neutron spectator, due to the quasi-free assumption [12]. The angular distributions test was performed for different ${}^6\text{Li}-\alpha$ relative energy intervals and normalized to the direct data [13,14]. An example of the result is shown in fig. 4. The error bars include both statistical and normalization errors. The two-body cross section is in arbitrary units and the solid lines show the behavior of direct angular distribution [13,14]. The quite fair agreement between the two trends makes us confident on the validity of the IA.

A second validity test consists in the comparison between the behavior of the indirect excitation function with the direct one. Therefore, by using the eq. (2), the quantity $(d\sigma/d\Omega)^{off}$ has been extracted. It has to be emphasized that in the present case the obtained cross section is the nuclear part, the Coulomb barrier being already overcome in entrance channel. In order to do the comparison the indirect two-body cross section was multiplied by Coulomb penetration function, given in terms of regular and irregular Coulomb functions (see [9,10,15] and references

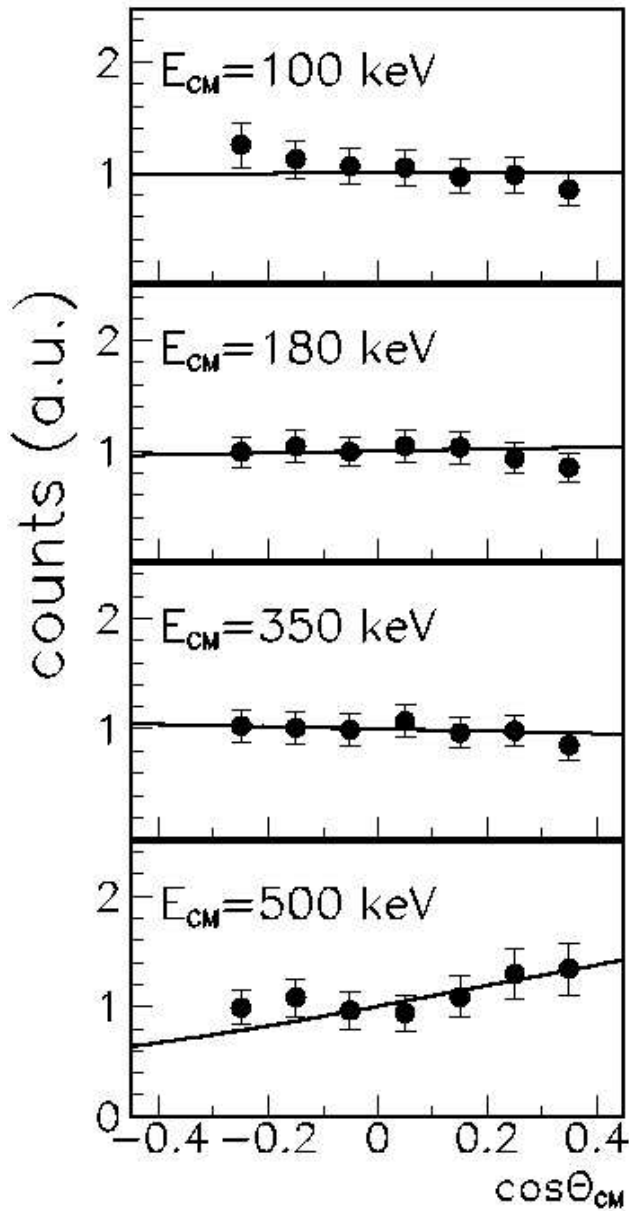


Fig. 4. Example of angular distribution extracted at different E_{cm} via the THM (dots) compared to the direct data (solid lines) [13,14].

therein). The resulting two-body cross-section $\sigma(E)$ is shown in fig. 5 (square symbols) where direct data [13] are also reported (dots). The normalization to direct behavior was performed in the region around $E_{cm} = 700$ keV. The good agreement between the two data sets is a necessary condition for the further extraction of the astrophysical $S(E)$ -factor by means of THM.

At the end of this second test on the data we can conclude that the PWIA analysis is able to correctly describe the studied process.

According to eq. (1) the bare-nucleus $S_b(E)$ -factor was extracted. The result is shown in fig. 6 and is compared

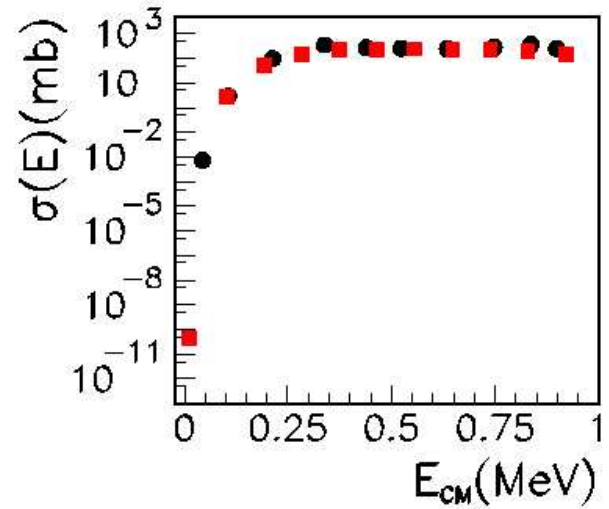


Fig. 5. Comparison between the THM indirect excitation function (square symbols) for the ${}^9\text{Be}(p, \alpha){}^6\text{Li}$ reaction and the direct behavior (dots) [13].

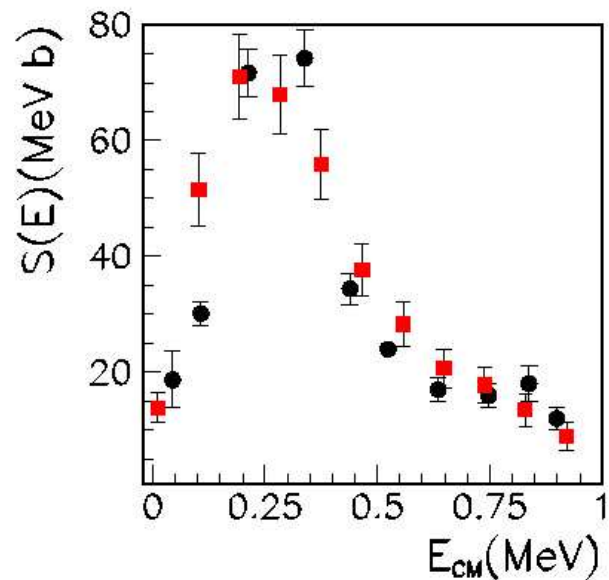


Fig. 6. The bare-nucleus astrophysical $S(E)$ -factor extracted via the THM (square symbols) compared with the direct one (dots) [13].

with direct data. Both sets of data were averaged out at the same energy bin of 90 keV.

5 Conclusion

The indirect study of the ${}^9\text{Be}(p, \alpha){}^6\text{Li}$ reaction was performed in the astrophysical energy region by applying the THM to the ${}^2\text{H}({}^9\text{Be}, {}^6\text{Li})n$ three-body break-up process. The results obtained represent an additional validity test of the method at sub-Coulomb energies. In particular the behavior of the indirect $S(E)$ -factor (fig. 6)

show the presence of the expected low-energy resonance at $E_{cm} \sim 0.27$ MeV, corresponding to the 6.87 MeV $J = 1^-$ level of ${}^{10}\text{B}$. It should be noticed that the resonance width in the indirect data is larger than in direct ones. This can be connected with the energy resolution (around 90 keV) of the present experiment which is poorer with respect to the direct one. This means that presently it is not possible to extract any information about screening effects. An upgraded experimental setup might improve the present results and give useful information for astrophysical applications.

References

1. R.N. Boyd, T. Kajino, *Astrophys. J.* **336**, L55 (1989).
2. A. Stephens *et al.*, *Astrophys. J.* **491**, 339 (1997).
3. C. Rolfs, W.S. Rodney, *Cauldrons in the Cosmos* (University of Chicago Press, Chicago, 1988).
4. G. Baur, H. Rebel, *J. Phys. G* **20**, 1 (1994) and references therein.
5. G. Baur, H. Rebel, *Annu. Rev. Nucl. Part. Sci.* **46**, 321 (1996).
6. A.M. Mukhamedzhanov *et al.*, *Phys. Rev. C* **56**, 1302 (1997).
7. A.M. Mukhamedzhanov *et al.*, *Phys. Rev. C* **63**, 024612 (2001).
8. G. Baur, *Phys. Lett. B* **178**, 135 (1986).
9. C. Spitaleri *et al.*, *Phys. Rev. C* **60**, 055802 (1999).
10. C. Spitaleri *et al.*, *Phys. Rev. C* **69**, 055806 (2004).
11. M. Zadro *et al.*, *Phys. Rev. C* **40**, 181 (1989).
12. M. Jain *et al.*, *Nucl. Phys. A* **153**, 49 (1970).
13. A.J. Sierk, T.A. Tombrello, *Nucl. Phys. A* **210**, 341 (1973).
14. D. Zahnw *et al.*, *Z. Phys. A* **359**, 211 (1997).
15. S. Typel, H. Wolter, *Few-Body Syst.* **29**, 7 (2000).